Non-monotonic feedback dependence on CO_2 due to a North Atlantic pattern effect

Ivan Mitevski[1], Yue Dong[2], Lorenzo M. Polvani[1,2], Maria Rugenstein[3], Clara Orbe[1,4]

[1]Department of Applied Physics and Applied Mathematics, Columbia University, New York, NY
[2]Lamont-Doherty Earth Observatory, Columbia University, Palisades, NY
[3]Department of Atmospheric Science, Colorado State University, Fort Collins, CO
[4]NASA Goddard Institute for Space Studies, New York, NY

Key Points:

- Effective climate sensitivity (EffCS) and radiative feedbacks change non-monotonically with increasing CO_2 concentrations
- The non-monotonicity is associated with the formation of a sea-surface temperature cooling pattern over the North Atlantic
- Results imply an overlooked radiative damping effect on global EffCS from the North Atlantic warming hole

Corresponding author: Ivan Mitevski, im2527@columbia.edu

Abstract

Effective climate sensitivity (EffCS), commonly estimated from model simulations with abrupt CO_2 quadrupling, has been shown to depend on the level of CO_2 forcing. To understand this dependency systematically, we performed a series of simulations with a range of abrupt CO_2 forcing in two climate models (CESM1-LE and GISS-E2.1-G). Our results indicate that EffCS is a non-monotonic function of the CO_2 forcing, decreasing between $3\times$ and $4\times CO_2$ in CESM1 ($2\times$ and $3\times CO_2$ in GISS) and increasing at higher CO_2 levels. The minimum EffCS value, caused by anomalously negative radiative feedbacks, arises from sea-surface temperature (SST) cooling in the North Atlantic. This localized North Atlantic cooling pattern is associated with the formation of the North Atlantic Warming Hole, accompanied by the collapse of the Atlantic Meridional Overturning Circulation under CO_2 forcing. Our findings emphasize the importance of understanding changes in North Atlantic SST patterns for constraining near-future and equilibrium global warming.

Plain Language Summary

Estimates of effective climate sensitivity (EffCS) are complicated by 1) the nonlinear dependence of feedback on temperature and 2) the sea-surface temperature (SST) pattern effect. We find that EffCS and radiative feedbacks change non-monotonically with CO_2 concentrations due to a cooling SST pattern over the North Atlantic associated with the formation of a “North Atlantic Warming Hole” (NAWH). While most previous studies focused on the impact of tropical Pacific SST patterns on EffCS, we here highlight an overlooked damping effect on EffCS from North Atlantic SST cooling across CO_2 levels. Our results imply that understanding and constraining the NAWH under CO_2 forcings is crucial for transient warming projections and EffCS constraints.

1 Introduction

Equilibrium climate sensitivity (ECS), the equilibrium global-mean surface air temperature response to a doubling of atmospheric CO_2 relative to pre-industrial (PI) levels, is one of the most important metrics in climate science. The Charney 1979 report estimated a “likely” ECS range of 1.5-4.5K; most recently, a tighter range of ECS values between 2.6-3.9K was established using a Bayesian framework that combines multiple lines of evidence (Sherwood et al., 2020).

When evaluated from climate models, ECS is often approximated with an effective climate sensitivity (EffCS), estimated from 150-year abrupt CO_2 quadrupling simulations within coupled global climate models (GCMs), with an underlying assumption that EffCS remains constant with different CO_2 doublings. However, previous modeling (Bloch-Johnson et al., 2021; Meraner et al., 2013; Mauritsen et al., 2019; Sherwood et al., 2020; Mitevski et al., 2021; Zhu & Poulsen, 2020) and paleoclimate studies (Anagnostou et al., 2016, 2020; Farnsworth et al., 2019; Friedrich et al., 2016; Shaffer et al., 2016; Zhu et al., 2019) have shown that EffCS may not be linear with each successive CO_2 doubling. It tends to increase at higher CO_2 values primarily due to a nonlinear temperature dependence of the radiative feedbacks (λ), referred to as the state-dependence of feedbacks (Andrews et al., 2015; Bloch-Johnson et al., 2021; Sherwood et al., 2015), with minor contributions from nonlinear CO_2 dependence of radiative forcing (Mitevski et al., 2022).

However, previous attempts to study the state dependence have been limited to CO_2-doubling scenarios ($2\times, 4\times, 8\times CO_2$) (Good et al., 2016; M. Rugenstein et al., 2019), whereas the shared socioeconomic pathway for the highest emission scenarios (SSP5-8.5) projects a transient increase of greenhouse gas forcing up to $8\times CO_2$ at the year 2300 (Meinshausen et al., 2020) passing through all the intermediate states of $n\times CO_2$ ($n = 2, 3, 4, 5, 6, 7, 8$). Moreover, previous studies have been focused on how EffCS and feedbacks vary in response to changes in global-mean temperatures under different CO_2 forcing (Meraner et al., 2013;

Caballero & Huber, 2013; Bloch-Johnson et al., 2021), with little attention on how the spatial patterns of feedback and local surface warming respond to various CO_2 forcings. Hence in this study, we examine the dependence of EffCS on CO_2 levels systematically and its connection to the spatial patterns of the climate feedbacks by performing and analyzing a hierarchy of GCM experiments with a range of abrupt CO_2 forcings including 2×, 3×, 4×, 5×, 6×, 7×, and 8×CO_2 relative to PI level (hereafter denoted as abrupt $n\times CO_2$ experiments).

2 Materials and Methods

2.1 Models and Experiments

We use the original large ensemble version of the Community Earth System Model (CESM1-LE). CESM1-LE comprises the Community Atmosphere Model version 5 (CAM5, 30 vertical levels) and parallel ocean program version 2 (POP2, 60 vertical levels) with approximately 1° horizontal resolution in all model components (Kay et al., 2015). Some of the results are shown with the GISS-E2.1-G model (Kelley et al., 2020) in Supplementary Information. All experiments in this work are with abrupt CO_2 forcing.

We perform abrupt $n\times CO_2$ experiments with the coupled version of the CESM1-LE and GISS-E2.1-G models (coupled runs) for 150 years with 2×, 3×, 4×, 5×, 6×, 7×, and 8×CO_2 forcing, with all other trace gases, aerosols, ozone concentrations, and solar forcing fixed at PI values. The response is defined as the difference between the $n\times CO_2$ runs and the PI control run. The same experiments were analyzed in (Mitevski et al., 2021, 2022).

To estimate the effective radiative forcing (ERF) as per Forster et al. (2016), we perform prescribed pre-industrial SST and sea-ice runs for 30 years for each 2×, 3×, 4×, 5×, 6×, 7×, and 8×CO_2. The ERF is then calculated as the global mean net top of the atmosphere (TOA) net radiation between PI and $n\times CO_2$, and it includes the stratospheric and tropospheric adjustments (Sherwood et al., 2015).

We also utilize atmosphere-only runs (AGCM) with prescribed monthly SST values taken from the 150-year abrupt $n\times CO_2$ runs. The prescribed SST values are monthly data for 150 years. The CO_2 concentration, ozone concentrations, aerosols, solar forcing, and all other trace gases are fixed at pre-industrial values.

In addition to only prescribing SST values from the $n\times CO_2$ runs, we also change the SST patterns. We use the pattern from 3×CO_2 in CESM1-LE and then scale the pattern by the global-mean warming amplitude from 4×CO_2 and 5×CO_2. We do this by

$$\Delta\mathrm{SST}(x,y,t) = \mathrm{SST}_{3\times\mathrm{CO_2}}(x,y,t) - \mathrm{SST}_{\mathrm{PI}}(x,y),$$

t is monthly data from 150 years, x is longitude, and y is latitude. Next, we find the pattern S_p as

$$S_p(x,y,t) = \frac{\Delta\mathrm{SST}(x,y,t)}{\overline{\Delta\mathrm{SST}}(t)}$$

where $\overline{\Delta\mathrm{SST}}$ is the global mean monthly data for 150 years. Then we have

$$\Delta\mathrm{SST}'_{n\times\mathrm{CO_2}}(x,y,t) = S_p \cdot \overline{\mathrm{SST}_{n\times\mathrm{CO_2}}}.$$

And finally

$$\mathrm{SST}_{n\times\mathrm{CO_2}}(x,y,t) = \mathrm{SST}_{PI}(x,y) + \Delta\mathrm{SST}'_{n\times\mathrm{CO_2}}(x,y,t).$$

One caveat here is that we are only changing the SSTs, and holding sea-ice fixed at 3×CO_2. Although sea-ice changes also cause albedo feedback changes, their contribution is much smaller than the SST-mediated feedback changes.

2.2 Analysis

We calculate the effective climate sensitivity EffCS as the x-intercept of regressing the change in net TOA radiation against surface air temperature over the 150 years of the simulations (Gregory et al., 2004; Zelinka et al., 2020). We normalize the EffCS by $\log_2 n$ for the $n\times CO_2$ runs, assuming logarithmic CO_2 forcing, consistent with Bloch-Johnson et al. (2021).

We calculate individual feedbacks with radiative kernels from Pendergrass et al. (2018). For each year, we multiply the spatially resolved kernels by the climate field anomalies of atmospheric temperature T, water vapor q, and surface albedo α. We regress these quantities on the surface temperature response, and the slope of this regression is the feedback. The cloud feedbacks are computed via the residual method (Soden & Held, 2006).

3 Results

3.1 Non-monotonic effective climate sensitivity and radiative feedbacks

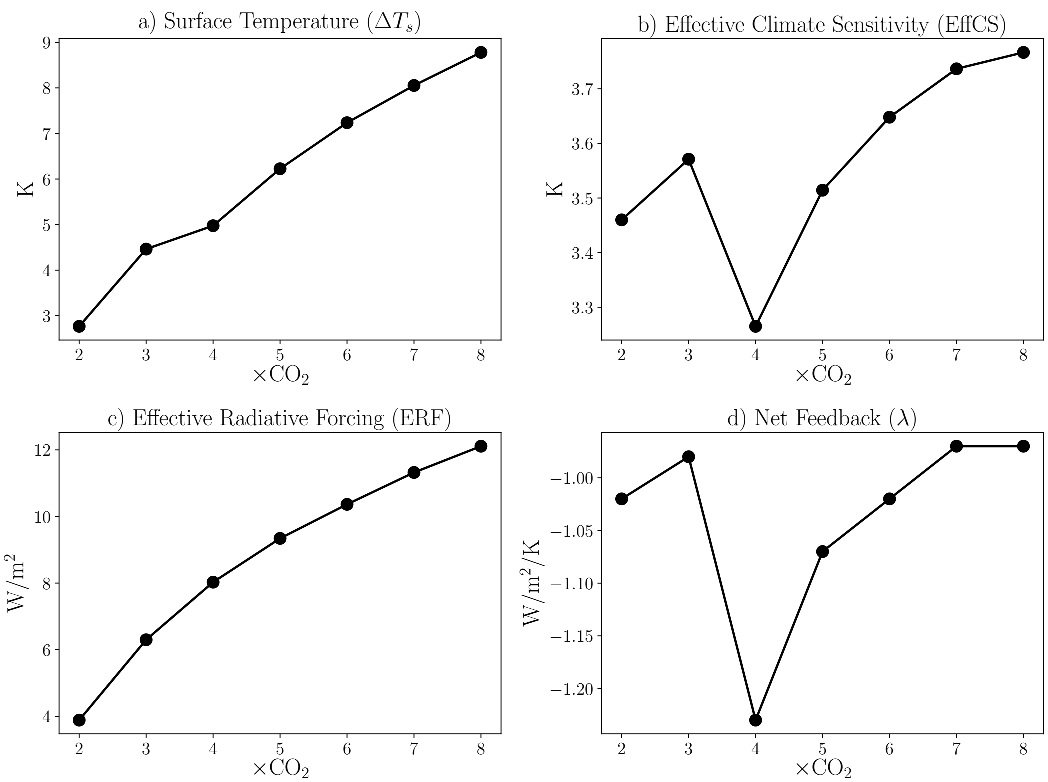

Figure 1. a) Global mean surface air temperature response (ΔT_s), b) effective climate sensitivity (EffCS), c) effective radiative forcing (ERF) from 30-year fixed sea-surface temperature runs, and d) net feedback parameter (λ) from the 150-year Gregory regression of abrupt $n\times CO_2$ runs.

Results from CESM1-LE show that although the global-mean surface air temperature increases monotonically as CO_2 increases (Fig. 1a), EffCS changes non-monotonically with CO_2 levels (Fig. 1b). That is, EffCS decreases between 3× and $4\times CO_2$ and then increases between 4× and $5\times CO_2$, and at higher CO_2 forcing, with a minimum value at $4\times CO_2$. We find the same non-monotonicity in the GISS-E2.1-G experiments except with a minimum EffCS at $3\times CO_2$ (Fig. S1). In the rest of the paper, we will focus on the CESM1-LE simulations and note that the results hold for the GISS-E2.1-G simulations unless otherwise noted.

Changes in EffCS, in principle, are governed by changes in effective radiative forcing (ERF) and radiative feedbacks (λ). While the ERF, calculated from an additional 30-year fixed sea-surface temperature (SST) runs as per Forster et al. (2016), increases slightly more than the logarithm of the CO_2 concentration at higher CO_2 levels than $4\times CO_2$ (see Mitevski et al. (2022) for more detail), it is strongly monotonic with CO_2 and does not exhibit a minimum value (Fig. 1c). On the other hand, the net radiative feedback parameter λ (Fig. 1d), calculated from 150-year regressions of top-of-atmosphere (TOA) radiative response against surface air temperature change (Zelinka et al., 2020), exhibits a clearly non-monotonic behavior with respect to CO_2 levels, as for EffCS: λ becomes more negative (more stabilizing) between $3\times$ and $4\times CO_2$ and less negative between $4\times$ and $5\times CO_2$, corresponding to the lowest EffCS at $4\times CO_2$. Similar results are also found in the GISS-E2.1-G model experiments (Fig. S1). These results suggest that EffCS depends not only *nonlinearly* on CO_2, as found in previous studies (Meraner et al., 2013; Caballero & Huber, 2013; Bloch-Johnson et al., 2021), but also *non-monotonically*, and that the non-monotonicity is caused by the radiative feedbacks in our simulations. Hence the question is: what causes the non-monotonic changes in feedbacks?

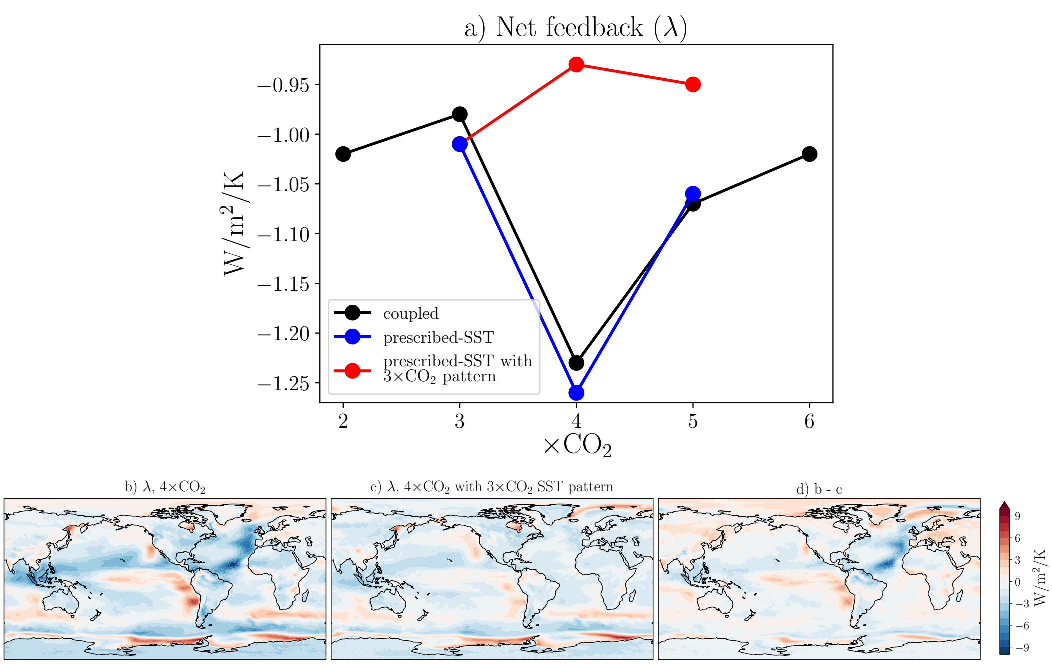

Figure 2. a) Global net feedback parameter λ from coupled runs, AGCM prescribed-SST runs with SSTs from coupled runs, and prescribed-SST runs with $3\times CO_2$ pattern, where the $3\times CO_2$ SST patterns are scaled with the actual global-mean SST values of $4\times CO_2$ and $5\times CO_2$, respectively. Spatial patterns of the local contribution to the global λ at $4\times CO_2$ from b) prescribed-SST, c) prescribed-SST with $3\times CO_2$ pattern and d) the difference.

3.2 Non-monotonic λ traced to changes in surface warming patterns

We hypothesize two reasons for the non-monotonic changes in λ with CO_2:

1. The non-monotonic dependence in λ may arise from a nonlinear state-dependence of the feedbacks. As noted above, previous studies have found that radiative feedbacks change nonlinearly with global-mean surface temperature changes (i.e., feedback temperature dependence), mostly owing to the cloud and water vapor feedbacks (Meraner et al., 2013; Caballero & Huber, 2013; Bloch-Johnson et al., 2021). Can the changes in global-mean surface temperature across the CO_2 levels in our simulations (Fig. 1a) explain the non-monotonic behavior of λ and, therefore, EffCS?
2. The non-monotonic dependence of λ may arise from a strong dependence of λ on the spatial pattern of SSTs. Recent studies have found a close coupling between SST patterns and radiative feedbacks in observations and model simulations, the so-called "pattern effect" (Zhou et al., 2016; Dong et al., 2019; Sherwood et al., 2020). If the SST pattern effect caused the non-monotonic response in λ, then what SST regions govern the global and local changes in our feedbacks?

To test the hypotheses, we run the atmospheric component of the coupled model CESM1-LE (CAM5) with specified SST boundary conditions, in order to examine the impacts of different surface warming on λ. First, we perform a set of 150-year long CAM5 simulations where we fix all radiative forcing agents at pre-industrial levels, and prescribe the time-varying SSTs produced by the corresponding coupled model $n \times CO_2$ simulations. In these runs (denoted as "prescribed-SST"), TOA radiative fluxes and surface air temperature freely adjust to the underlying SSTs. Although not directly forced by CO_2, we find that the prescribed-SST simulations accurately reproduce the values of λ from the corresponding coupled simulations (c.f. blue and black dots in Fig. 2a). This finding, consistent with other studies (Haugstad et al., 2017; Zhou et al., 2023), suggests that the dependence of λ on CO_2 forcing is primarily shaped by the SSTs induced by the CO_2 forcing and therefore confirms the validity of using prescribed-SST simulations to study radiative feedbacks to understand the coupled $n\times CO_2$ results.

Next, we perform another set of prescribed-SST simulations with adjusted SST boundary conditions. To test hypothesis # 1, i.e., whether λ responds non-monotonically to changes in global-mean surface temperatures, we conduct simulations where we scale the SST pattern from $3\times CO_2$ by the actual global-mean SST changes in coupled $4\times CO_2$ and $5\times CO_2$, respectively. Such that these two runs have the same normalized global SST pattern (at every monthly time step) as the $3\times CO_2$ run but different global-mean SST values (denoted "prescribed-SST with $3\times CO_2$ pattern"). In these experiments, we find that the λ values do not reproduce those in the coupled & prescribed-SST simulations even though the same global-mean SST warming is prescribed (c.f. red and blue dots in Fig. 2a), suggesting that the non-monotonic response in λ arises from changes in the spatial pattern of SSTs (hypothesis # 2) and not the changes in the global-mean values of SSTs (hypothesis # 1).

The above CAM5 prescribed-SST simulations highlight the role of SST patterns in driving the non-monotonic response in λ. To understand what regions contribute to this non-monotonicity, we show the spatial pattern of λ calculated as the local net TOA radiation regressed to global-mean surface air temperature response, shown in Fig. 2b-d. The spatial pattern of λ in the $4\times CO_2$ prescribed-SST run ($4\times CO_2$ SST pattern), is shown in Fig. 2b, corresponding to the globally averaged λ at $4\times CO_2$ shown by the blue dot in Fig. 2a. The spatial pattern of λ in a $4\times CO_2$ run with $3\times CO_2$ SST pattern (red dot in Fig. 2a) is shown in Fig. 2c. Taking the difference between Fig. 2b and c (panel d) shows substantially more negative feedback in the North Atlantic with the $4\times CO_2$ pattern, and not much change when we use the $3\times CO_2$ pattern, indicating that the anomalously low EffCS at $4\times CO_2$ in our coupled simulations is primarily associated with an anomalously negative λ in the North Atlantic.

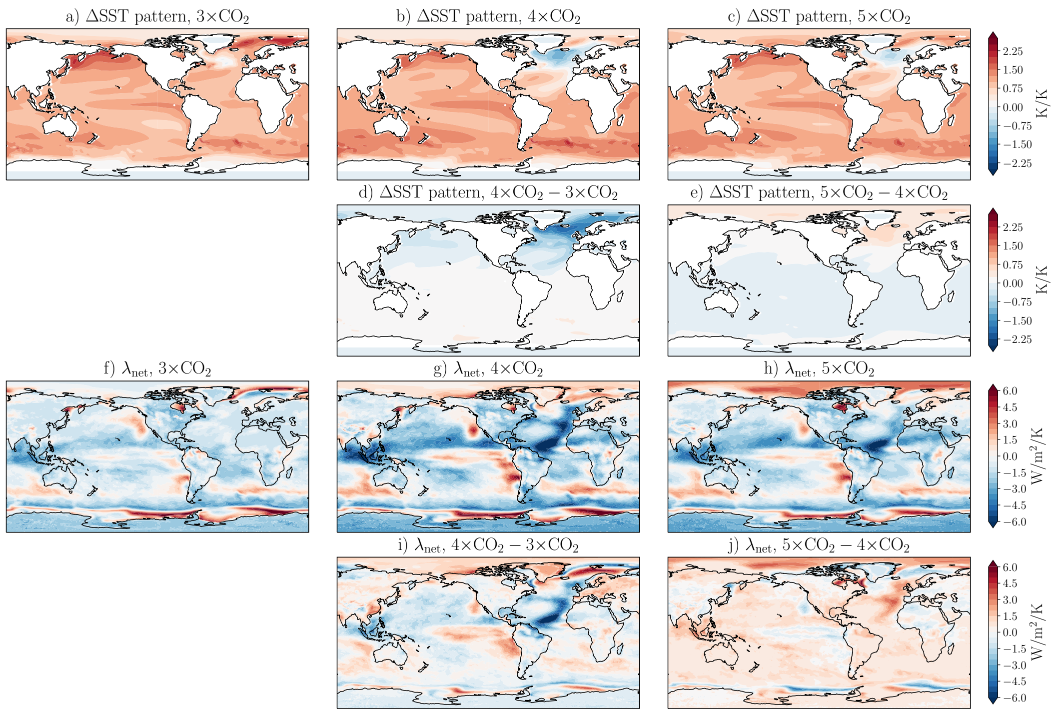

Figure 3. Maps of SST patterns (calculated as the regression of local temperature changes to global temperature changes for 150 years) in the coupled runs for a) $3\times CO_2$, b) $4\times CO_2$, and c) $5\times CO_2$. The differences between $4\times$ and $3\times CO_2$, and $5\times$ and $4\times CO_2$, are shown in d) and e), respectively. Figures f-j) show λ maps for the same CO_2 experiments.

3.3 A local pattern effect from the North Atlantic

While the stronger negative feedbacks appear to be located mainly in the North Atlantic, it is unclear whether they are driven by the local North Atlantic SST changes, or by remote SST impacts from other basins. In Fig. 3, we show the normalized SST patterns (over the full 150 years of the simulations) from $3\times$, $4\times$, and $5\times CO_2$ simulations (panels a-c). We find that anomalous SST cooling primarily occurs in the North Atlantic: $4\times CO_2$ produces a strong cooling pattern in the North Atlantic, largely resembling the pattern of the North Atlantic Warming Hole (NAWH) (Chemke et al., 2020). However, this North Atlantic relative-cooling pattern does not emerge at $3\times CO_2$ (panel a) and is much weaker at $5\times CO_2$ (panel c). Concurrently, we find that local feedbacks exhibit patterns that closely match the SST patterns (Fig. 3f,g, and h). Most of the strengthening of negative feedback that would result in lower EffCS is found at $4\times$ relative to $3\times CO_2$ (Fig. 3i), and it occurs in the North Atlantic, corresponding with the local cooling pattern (Fig. 3d); while most of the weakening of feedbacks at $5\times$ relative to $4\times CO_2$ (higher EffCS, Fig. 3j) which also occurs in the North Atlantic, corresponds with the local warming pattern (Fig. 3e). These results suggest that the non-monotonic response of the feedbacks found in our simulations (Fig. 2a) is predominately from feedback changes in the North Atlantic, associated with North Atlantic local SST changes. We note that significant feedback changes also occur in the tropical Pacific (Fig. 3i,j), particularly the tropical Eastern Pacific, but these feedback changes are in the opposite sign to the global-mean feedback changes, and thus cannot account for the total feedback response we showed in Fig. 2a. While some other regions may contribute to the negative feedback change (e.g., the tropical Western Pacific and the Southern Ocean), we find that the North Atlantic local λ (area between 0 to 60N and 80W to 10E) explains up to 2/3 of the total change in the global-mean λ (Fig. S2). This suggests that most of the non-monotonicity at $4\times CO_2$ is due to the North Atlantic pattern effect.

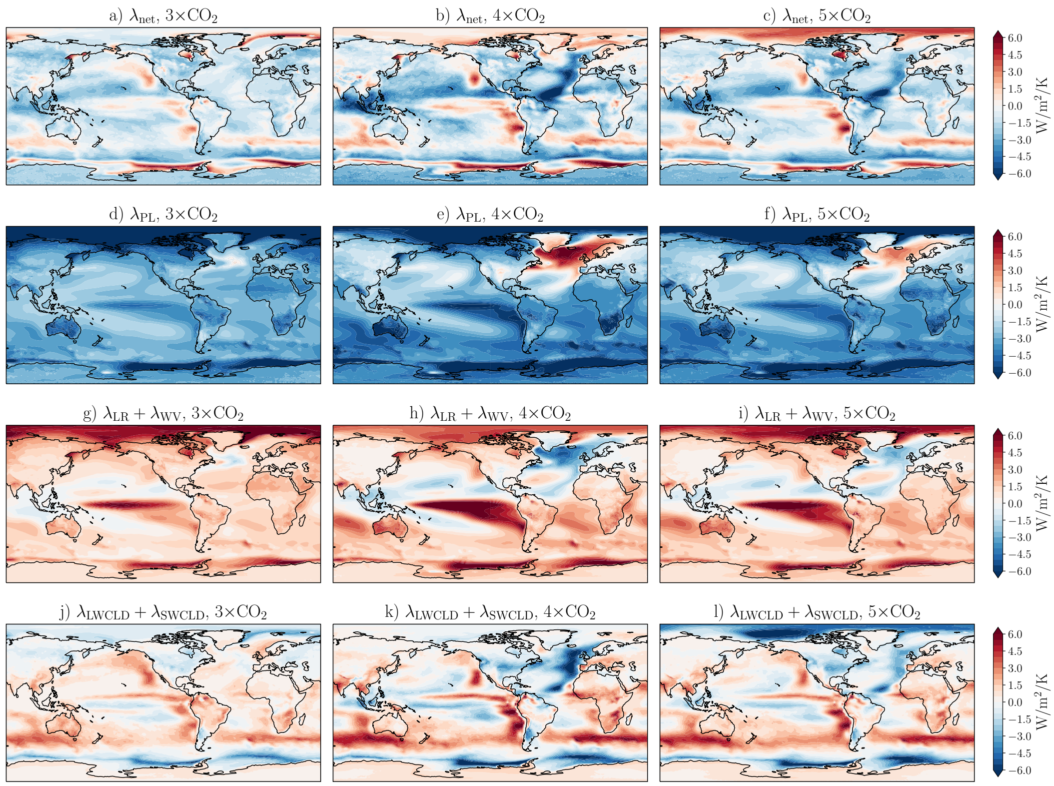

Figure 4. Maps of individual feedbacks calculated from prescribed-SST runs for: a-c) net, d-f) Planck, g-i) lapse rate + water vapor, j-i) net cloud.

To further understand the processes causing the λ non-monotonicity, we further decompose the net feedback parameter λ into the individual feedbacks using radiative kernels (Pendergrass et al., 2018) (Fig. 4). In the North Atlantic at $4\times CO_2$, the Planck feedback (Fig. 4e) is strongly positive as the local cooling reduces outgoing radiation, whereas the combined lapse rate and water vapor feedback (Fig. 4h) and the cloud feedback (Fig. 4k) contribute negatively. The strong negative feedback at $4\times CO_2$ compared to $3\times CO_2$ in the subtropical North Atlantic is primarily due to the SW cloud feedback (Fig. S2 and Fig. S3h); hence, it is one of the key contributors to the λ non-monotonicity at $4\times CO_2$. This is because local cooling strengthens lower tropospheric stability (often measured as estimated inversion strength (EIS)), which increases low-cloud cover (negative cloud feedback) and more-negative lapse rate feedback. This mechanism is consistent with the leading mechanism found in the tropical Pacific pattern effect (Zhou et al., 2016; Andrews & Webb, 2018; Dong et al., 2019), except this pattern effect here is associated with the North Atlantic SST changes (Lin et al., 2019), and causes the non-monotonic response in EffCS and λ across CO_2 levels in our experiments. We refer the reader to Lin et al. (2019) for more details on this mechanism. Additionally, it is important to note that 2/3 of the difference in feedbacks between $4\times CO_2$ and $3\times CO_2$ comes from the North Atlantic and 1/3 from the rest of the globe. At $4\times CO_2$, there are strong responses in the individual feedbacks in the tropical Pacific (see Fig. S3 for albedo and longwave cloud feedbacks). However, the negative Planck feedback response in the tropical Pacific is compensated by the local positive feedback response from lapse rate, water vapor, and clouds (Fig. 4b,e,h,k), which makes the tropical Pacific less pronounced in the λ non-monotonic changes.

Having shown that feedback changes primarily come from the North Atlantic associated with local SST cooling, we finally return to the key pattern of North Atlantic SST cooling found in our simulations, the North Atlantic warming hole (NAWH). In the literature, the appearance of the NAWH has been attributed to the slowdown in the AMOC and linked to an atmospheric response (Rahmstorf et al., 2015; Sévellec et al., 2017; Caesar et al., 2018; Latif et al., 2022). Our previous work (Fig. S3 in (Mitevski et al., 2021)) found the North Atlantic cooling (NAWH) in our experiments is primarily due to AMOC collapse. The AMOC collapses at 4×CO_2 in our GCM, and at all other higher CO_2 forcings. At higher CO_2 forcings (5×CO_2 and above), the AMOC collapse no longer produces anomalous North Atlantic cooling compared to the previous level of CO_2 forcing (e.g., 4×CO_2) because the AMOC collapse-induced SST cooling is further overwhelmed by the surrounding warming. Hence, the cooling over the NAWH is less pronounced at higher CO_2 forcings (Fig. 3c) and has a smaller impact on the feedbacks (Fig. 3h). The collapse of the AMOC under CO_2 forcing has been widely reported in climate models, including the GISS-E2.1-G model in this study (occurring at 3×CO_2 & higher) and many other CMIP5 and CMIP6 models (Fig. S3 in (Mitevski et al., 2021)).

4 Discussion and Conclusion

In a series of $n\times CO_2$ ($n = 2, 3, 4, 5, 6, 7, 8$) experiments, we find a non-monotonic response in the effective climate sensitivity (EffCS) to CO_2 forcing using two state-of-the-art, coupled climate models. EffCS becomes anomalously low at an intermediate level of CO_2 (4×CO_2 in CESM1-LE and 3×CO_2 in GISS-E2.1-G) but increases at higher CO_2 levels. This EffCS non-monotonicity is primarily linked to changes in radiative feedback λ due to North Atlantic cooling; λ becomes anomalously negative when cooling emerges in the North Atlantic and forms a North Atlantic Warming Hole (NAWH).

The dependence of λ on sea-surface temperature (SST) patterns has been widely studied, with a focus on the time-evolution of those patterns (Andrews et al., 2015; Zhou et al., 2016; Dong et al., 2019; Andrews et al., 2022; Sherwood et al., 2020). For example, estimates of EffCS from the observed historical energy budget constraints are lower than those from long-term warming under CO_2 quadrupling, primarily owing to changes in the tropical Pacific SST patterns (Zhou et al., 2016; Dong et al., 2019; Andrews et al., 2018, 2022; Gregory et al., 2020). This "pattern effect" has been studied with a Green's function approach (Dong et al., 2019; Zhou et al., 2017; Zhang et al., 2023), which shows that the global feedback has a predominant dependence on tropical western Pacific SSTs and is less sensitive to the North Atlantic SSTs. This tropical Pacific SST pattern effect has been found to be a leading mechanism for the time evolution of EffCS estimates. However, our study proposes a new North Atlantic pattern effect that accounts for changes in EffCS and feedbacks across different CO_2 forcing levels. This North Atlantic pattern effect shows that SST cooling in the North Atlantic due to the formation of NAWH causes λ to become more negative and, therefore, lower EffCS. We note that the North Atlantic pattern effect operates on the dimension of increasing CO_2 forcing, instead of on the dimension of time evolution reported in previous studies (Dong et al., 2019; Andrews & Webb, 2018; Andrews et al., 2022; Zhou et al., 2016).

The NAWH has been proposed to arise from the reduction of surface meridional ocean heat transport (Chemke et al., 2020) or AMOC slowdown that reduces transient warming due to increased ocean heat uptake (Caesar et al., 2020; Palter, 2015; M. A. Rugenstein et al., 2013; Trossman et al., 2016; Winton et al., 2013). In our study, we find that the NAWH can further reduce EffCS and transient warming by causing more negative feedback (more efficient radiative damping at the top of the atmosphere). The fact that the NAWH has been observed in the historical period and is projected to persist in future scenarios with increasing GHG (Menary & Wood, 2018; Chemke et al., 2020; Keil et al., 2020; Gervais et al., 2018; Liu et al., 2020; Ren & Liu, 2021) suggests a considerable damping effect on future global warming from the North Atlantic, which may have been overlooked in the literature.

We further analyzed two subsets of CMIP6 models with and without NAWH in the abrupt-4×CO_2 runs (Fig. S4). Models with NAWH in the abrupt-4×CO_2 scenario also show more surface cooling in the North Atlantic in transient 21st-century simulations (under both SSP5-8.5 and SSP2-4.5 scenarios) than models without NAWH. This suggests that uncertainty in the projected long-term North Atlantic SST patterns in response to abrupt CO_2 forcing also persists in transient projections. Thus, understanding North Atlantic SST changes is crucial for constraining global climate change at both transient and equilibrium timescales.

One caveat to our findings is that the AMOC collapse in our models occurs at 3× and 4×CO_2, which are relatively low CO_2 values, where the collapse can induce a substantial cooling in the North Atlantic. When the AMOC collapses at a low CO_2 value, such as 2× or 3×CO_2, the North Atlantic cooling is strong, leading to a considerable non-monotonicity in EffCS. However, if the AMOC collapses at a higher CO_2 value, such as 5×CO_2, then the overwhelming CO_2 warming from the surrounding areas results in a weaker North Atlantic SST cooling pattern. In this case, the EffCS non-monotonicity would be smaller than the one reported in this study. Hence our results suggest that future changes in AMOC and NAWH may add additional uncertainty to EffCS and transient 21st century warming projections. Finally, we recognize that our results are obtained using only two GCMs. It would be important to repeat the same exercise with a broad range of models to test the robustness of our results.

The fact that EffCS is nonlinear and even non-monotonic with respect to CO_2 levels complicates equilibrium climate sensitivity constraints using models, observations, the paleoclimate record, and process-based understanding. While the non-constant λ across different CO_2 levels has been mainly attributed to feedback temperature dependence within models (Bloch-Johnson et al., 2021; Meraner et al., 2013; Mauritsen et al., 2019; Sherwood et al., 2020; Zhu & Poulsen, 2020) and paleoclimate records (Anagnostou et al., 2016, 2020; Farnsworth et al., 2019; Friedrich et al., 2016; Shaffer et al., 2016; Zhu et al., 2019), we here have shown that the SST pattern also plays a role. Our study adds additional evidence of EffCS state dependence and pattern effects, which need to be further examined in other lines of evidence.

5 Open Research Section

Part of the computing and data storage resources, including the Cheyenne supercomputer (`https://doi.org/10.5065/D6RX99HX`), were provided by the Computational and Information Systems Laboratory at National Center for Atmospheric Research (NCAR). The CESM-LE model data can be obtained at `https://doi.org/10.5281/zenodo.5725084` and GISS-E2.1-G model data at `https://doi.org/10.5281/zenodo.3901624`.

Acknowledgments

This work was supported by NASA FINESST Grant 80NSSC20K1657. YD was supported by the NOAA Climate and Global Change Postdoctoral Fellowship Program, administered by UCAR's Cooperative Programs for the Advancement of Earth System Science (CPAESS) under award NA210AR4310383. MR was supported by the National Science Foundation under Grant No. 2202916. The work of LMP is supported, in part, by a grant from the US National Science Foundation to Columbia University. We thank the high-performance computing resources provided by NASA's Advanced Supercomputing (NAS) Division and the NASA Center for Climate Simulation (NCCS).

References

Anagnostou, E., John, E. H., Babila, T. L., Sexton, P. F., Ridgwell, A., Lunt, D. J., … Foster, G. L. (2020, Sep 07). Proxy evidence for state-dependence of climate sensitivity in the eocene greenhouse. *Nature Communications*, *11*(1), 4436. doi: https://doi.org/10.1038/s41467-020-17887-x

Anagnostou, E., John, E. H., Edgar, K. M., Foster, G. L., Ridgwell, A., Inglis, G. N., ... Pearson, P. N. (2016, May 01). Changing atmospheric co2 concentration was the primary driver of early cenozoic climate. *Nature*, *533*(7603), 380-384. doi: https://doi.org/10.1038/nature17423

Andrews, T., Bodas-Salcedo, A., Gregory, J. M., Dong, Y., Armour, K. C., Paynter, D., ... Liu, C. (2022). On the effect of historical sst patterns on radiative feedback. *Journal of Geophysical Research: Atmospheres*, *127*(18), e2022JD036675. doi: https://doi.org/10.1029/2022JD036675

Andrews, T., Gregory, J. M., Paynter, D., Silvers, L. G., Zhou, C., Mauritsen, T., ... Titchner, H. (2018). Accounting for changing temperature patterns increases historical estimates of climate sensitivity. *Geophysical Research Letters*, *45*(16), 8490-8499. Retrieved from `https://agupubs.onlinelibrary.wiley.com/doi/abs/10.1029/2018GL078887` doi: https://doi.org/10.1029/2018GL078887

Andrews, T., Gregory, J. M., & Webb, M. J. (2015). The dependence of radiative forcing and feedback on evolving patterns of surface temperature change in climate models. *Journal of Climate*, *28*(4), 1630 - 1648. Retrieved from `https://journals.ametsoc.org/view/journals/clim/28/4/jcli-d-14-00545.1.xml` doi: 10.1175/JCLI-D-14-00545.1

Andrews, T., & Webb, M. J. (2018). The dependence of global cloud and lapse rate feedbacks on the spatial structure of tropical pacific warming. *Journal of Climate*, *31*(2), 641 - 654. Retrieved from `https://journals.ametsoc.org/view/journals/clim/31/2/jcli-d-17-0087.1.xml` doi: https://doi.org/10.1175/JCLI-D-17-0087.1

Bloch-Johnson, J., Rugenstein, M., Stolpe, M. B., Rohrschneider, T., Zheng, Y., & Gregory, J. M. (2021). Climate sensitivity increases under higher co2 levels due to feedback temperature dependence. *Geophysical Research Letters*, *48*(4), e2020GL089074. Retrieved from `https://agupubs.onlinelibrary.wiley.com/doi/abs/10.1029/2020GL089074` (e2020GL089074 2020GL089074) doi: https://doi.org/10.1029/2020GL089074

Caballero, R., & Huber, M. (2013). State-dependent climate sensitivity in past warm climates and its implications for future climate projections. *Proceedings of the National Academy of Sciences*, *110*(35), 14162–14167. doi: 10.1073/pnas.1303365110

Caesar, L., Rahmstorf, S., & Feulner, G. (2020, jan). On the relationship between Atlantic meridional overturning circulation slowdown and global surface warming. *Environmental Research Letters*, *15*(2), 024003. doi: 10.1088/1748-9326/ab63e3

Caesar, L., Rahmstorf, S., Robinson, A., Feulner, G., & Saba, V. (2018, Apr 01). Observed fingerprint of a weakening atlantic ocean overturning circulation. *Nature*, *556*(7700), 191-196. Retrieved from `https://doi.org/10.1038/s41586-018-0006-5` doi: 10.1038/s41586-018-0006-5

Chemke, R., Zanna, L., & Polvani, L. M. (2020, Mar 24). Identifying a human signal in the north atlantic warming hole. *Nature Communications*, *11*(1), 1540. Retrieved from `https://doi.org/10.1038/s41467-020-15285-x` doi: 10.1038/s41467-020-15285-x

Dong, Y., Proistosescu, C., Armour, K. C., & Battisti, D. S. (2019). Attributing historical and future evolution of radiative feedbacks to regional warming patterns using a green's function approach: The preeminence of the western pacific. *Journal of Climate*, *32*(17), 5471 - 5491. Retrieved from `https://journals.ametsoc.org/view/journals/clim/32/17/jcli-d-18-0843.1.xml` doi: 10.1175/JCLI-D-18-0843.1

Farnsworth, A., Lunt, D. J., O'Brien, C. L., Foster, G. L., Inglis, G. N., Markwick, P., ... Robinson, S. A. (2019). Climate sensitivity on geological timescales controlled by nonlinear feedbacks and ocean circulation. *Geophysical Research Letters*, *46*(16), 9880-9889. doi: https://doi.org/10.1029/2019GL083574

Forster, P., Richardson, T., Maycock, A. C., Smith, C. J., Samset, B. H., Myhre, G., ... Schulz, M. (2016). Recommendations for diagnosing effective radiative forcing from climate models for CMIP6. *Journal of Geophysical Research: Atmospheres*, *121*(20), 12,460-12,475. doi: https://doi.org/10.1002/2016JD025320

Friedrich, T., Timmermann, A., Tigchelaar, M., Elison Timm, O., & Ganopolski, A. (2016). Nonlinear climate sensitivity and its implications for future greenhouse warming. *Science Advances*, *2*(11). doi: https://doi.org/10.1126/sciadv.1501923

Gervais, M., Shaman, J., & Kushnir, Y. (2018). Mechanisms governing the development of the north atlantic warming hole in the cesm-le future climate simulations. *Journal of Climate*, *31*(15), 5927 - 5946. Retrieved from `https://journals.ametsoc.org/view/journals/clim/31/15/jcli-d-17-0635.1.xml` doi: 10.1175/JCLI-D-17-0635.1

Good, P., Andrews, T., Chadwick, R., Dufresne, J.-L., Gregory, J. M., Lowe, J. A., ... Shiogama, H. (2016). nonlinmip contribution to CMIP6: model intercomparison project for non-linear mechanisms: physical basis, experimental design and analysis principles (v1.0). *Geoscientific Model Development*, *9*(11), 4019–4028. Retrieved from `https://gmd.copernicus.org/articles/9/4019/2016/` doi: 10.5194/gmd-9-4019-2016

Gregory, J., Andrews, T., Ceppi, P., Mauritsen, T., & Webb, M. (2020). How accurately can the climate sensitivity to co2 be estimated from historical climate change? *Climate Dynamics*, *54*(1), 129–157.

Gregory, J., Ingram, W. J., Palmer, M. A., Jones, G. S., Stott, P. A., Thorpe, R. B., ... Williams, K. D. (2004). A new method for diagnosing radiative forcing and climate sensitivity. *Geophysical Research Letters*, *31*(3). doi: https://doi.org/10.1029/2003GL018747

Haugstad, A. D., Armour, K. C., Battisti, D. S., & Rose, B. E. J. (2017). Relative roles of surface temperature and climate forcing patterns in the inconstancy of radiative feedbacks. *Geophysical Research Letters*, *44*(14), 7455-7463. Retrieved from `https://agupubs.onlinelibrary.wiley.com/doi/abs/10.1002/2017GL074372` doi: https://doi.org/10.1002/2017GL074372

Kay, J. E., Deser, C., Phillips, A., Mai, A., Hannay, C., Strand, G., ... Vertenstein, M. (2015, 09). The Community Earth System Model (CESM) Large Ensemble Project: A Community Resource for Studying Climate Change in the Presence of Internal Climate Variability. *Bulletin of the American Meteorological Society*, *96*(8), 1333-1349. doi: 10.1175/BAMS-D-13-00255.1

Keil, P., Mauritsen, T., Jungclaus, J., Hedemann, C., Olonscheck, D., & Ghosh, R. (2020, Jul 01). Multiple drivers of the north atlantic warming hole. *Nature Climate Change*, *10*(7), 667-671. Retrieved from `https://doi.org/10.1038/s41558-020-0819-8` doi: 10.1038/s41558-020-0819-8

Kelley, M., Schmidt, G. A., Nazarenko, L. S., Bauer, S. E., Ruedy, R., Russell, G. L., ... Yao, M.-S. (2020). Giss-e2.1: Configurations and climatology. *Journal of Advances in Modeling Earth Systems*, *12*(8), e2019MS002025. doi: https://doi.org/10.1029/2019MS002025

Latif, M., Sun, J., Visbeck, M., & Hadi Bordbar, M. (2022, May 01). Natural variability has dominated atlantic meridional overturning circulation since 1900. *Nature Climate Change*, *12*(5), 455-460. Retrieved from `https://doi.org/10.1038/s41558-022-01342-4` doi: 10.1038/s41558-022-01342-4

Lin, Y.-J., Hwang, Y.-T., Ceppi, P., & Gregory, J. M. (2019). Uncertainty in the evolution of climate feedback traced to the strength of the atlantic meridional overturning circulation. *Geophysical Research Letters*, *46*(21), 12331-12339. doi: https://doi.org/10.1029/2019GL083084

Liu, W., Fedorov, A. V., Xie, S.-P., & Hu, S. (2020). Climate impacts of a weakened atlantic meridional overturning circulation in a warming climate. *Science Advances*, *6*(26), eaaz4876. doi: 10.1126/sciadv.aaz4876

Mauritsen, T., Bader, J., Becker, T., Behrens, J., Bittner, M., Brokopf, R., ... Roeckner, E. (2019). Developments in the mpi-m earth system model version 1.2 (mpi-esm1.2) and its response to increasing co2. *Journal of Advances in Modeling Earth Systems*, *11*(4), 998-1038. doi: https://doi.org/10.1029/2018MS001400

Meinshausen, M., Nicholls, Z. R. J., Lewis, J., Gidden, M. J., Vogel, E., Freund, M.,

... Wang, R. H. J. (2020). The shared socio-economic pathway (ssp) greenhouse gas concentrations and their extensions to 2500. *Geoscientific Model Development*, *13*(8), 3571–3605. Retrieved from https://gmd.copernicus.org/articles/13/3571/2020/ doi: 10.5194/gmd-13-3571-2020

Menary, M. B., & Wood, R. A. (2018, Apr 01). An anatomy of the projected north atlantic warming hole in CMIP5 models. *Climate Dynamics*, *50*(7), 3063-3080. Retrieved from https://doi.org/10.1007/s00382-017-3793-8 doi: 10.1007/s00382-017-3793-8

Meraner, K., Mauritsen, T., & Voigt, A. (2013). robust increase in equilibrium climate sensitivity under global warming. *geophysical research letters*, *40*(22), 5944-5948. doi: https://doi.org/10.1002/2013gl058118

Mitevski, I., Orbe, C., Chemke, R., Nazarenko, L., & Polvani, L. M. (2021). Non-monotonic response of the climate system to abrupt co2 forcing. *Geophysical Research Letters*, *48*(6), e2020GL090861. doi: https://doi.org/10.1029/2020GL090861

Mitevski, I., Polvani, L. M., & Orbe, C. (2022). Asymmetric warming/cooling response to co2 increase/ decrease mainly due to non-logarithmic forcing, not feedbacks. *Geophysical Research Letters*, *49*, e2021GL097133. doi: https://doi.org/10.1029/2021GL097133

Palter, J. B. (2015). The Role of the Gulf Stream in European Climate. *Annual Review of Marine Science*, *7*(1), 113-137. doi: 10.1146/annurev-marine-010814-015656

Pendergrass, A. G., Conley, A., & Vitt, F. M. (2018). Surface and top-of-atmosphere radiative feedback kernels for cesm-cam5. *Earth System Science Data*, *10*(1), 317–324. Retrieved from https://essd.copernicus.org/articles/10/317/2018/ doi: 10.5194/essd-10-317-2018

Rahmstorf, S., Box, J. E., Feulner, G., Mann, M. E., Robinson, A., Rutherford, S., & Schaffernicht, E. J. (2015, May 01). Exceptional twentieth-century slowdown in atlantic ocean overturning circulation. *Nature Climate Change*, *5*(5), 475-480. Retrieved from https://doi.org/10.1038/nclimate2554 doi: 10.1038/nclimate2554

Ren, X., & Liu, W. (2021). The role of a weakened atlantic meridional overturning circulation in modulating marine heatwaves in a warming climate. *Geophysical Research Letters*, *48*(23), e2021GL095941. (e2021GL095941 2021GL095941) doi: https://doi.org/10.1029/2021GL095941

Rugenstein, M., Bloch-Johnson, J., Abe-Ouchi, A., Andrews, T., Beyerle, U., Cao, L., ... Yang, S. (2019). Longrunmip: Motivation and design for a large collection of millennial-length aogcm simulations. *Bulletin of the American Meteorological Society*, *100*(12), 2551 - 2570. Retrieved from https://journals.ametsoc.org/view/journals/bams/100/12/bams-d-19-0068.1.xml doi: 10.1175/BAMS-D-19-0068.1

Rugenstein, M. A., Winton, M., Stouffer, R. J., Griffies, S. M., & Hallberg, R. (2013, 01). Northern High-Latitude Heat Budget Decomposition and Transient Warming. *Journal of Climate*, *26*(2), 609-621. doi: 10.1175/JCLI-D-11-00695.1

Sévellec, F., Fedorov, A. V., & Liu, W. (2017, Aug 01). Arctic sea-ice decline weakens the atlantic meridional overturning circulation. *Nature Climate Change*, *7*(8), 604-610. Retrieved from https://doi.org/10.1038/nclimate3353 doi: 10.1038/nclimate3353

Shaffer, G., Huber, M., Rondanelli, R., & Pepke Pedersen, J. O. (2016). Deep time evidence for climate sensitivity increase with warming. *Geophysical Research Letters*, *43*(12), 6538-6545. doi: https://doi.org/10.1002/2016GL069243

Sherwood, S. C., Bony, S., Boucher, O., Bretherton, C., Forster, P. M., Gregory, J. M., & Stevens, B. (2015). Adjustments in the forcing-feedback framework for understanding climate change. *Bulletin of the American Meteorological Society*, *96*(2), 217-228. doi: 10.1175/BAMS-D-13-00167.1

Sherwood, S. C., Webb, M. J., Annan, J. D., Armour, K. C., Forster, P. M., Hargreaves, J. C., ... Zelinka, M. D. (2020). An assessment of earth's climate sensitivity using multiple lines of evidence. *Reviews of Geophysics*. doi: https://doi.org/10.1029/2019RG000678

Soden, B. J., & Held, I. M. (2006). An assessment of climate feedbacks in coupled ocean–atmosphere models. *Journal of Climate*, *19*(14), 3354 -

3360. Retrieved from https://journals.ametsoc.org/view/journals/clim/19/14/jcli3799.1.xml doi: 10.1175/JCLI3799.1
Trossman, D. S., Palter, J. B., Merlis, T. M., Huang, Y., & Xia, Y. (2016). Large-scale ocean circulation-cloud interactions reduce the pace of transient climate change. *Geophysical Research Letters*, *43*(8), 3935-3943. doi: 10.1002/2016GL067931
Winton, M., Griffies, S. M., Samuels, B. L., Sarmiento, J. L., & Frölicher, T. L. (2013, 04). Connecting Changing Ocean Circulation with Changing Climate. *Journal of Climate*, *26*(7), 2268-2278. doi: 10.1175/JCLI-D-12-00296.1
Zelinka, M. D., Myers, T. A., McCoy, D. T., Po-Chedley, S., Caldwell, P. M., Ceppi, P., ... Taylor, K. E. (2020). Causes of higher climate sensitivity in CMIP6 models. *Geophysical Research Letters*, *47*(1), e2019GL085782. Retrieved from https://agupubs.onlinelibrary.wiley.com/doi/abs/10.1029/2019GL085782 (e2019GL085782 10.1029/2019GL085782) doi: https://doi.org/10.1029/2019GL085782
Zhang, B., Zhao, M., & Tan, Z. (2023). Using a green's function approach to diagnose the pattern effect in gfdl am4 and cm4. *Journal of Climate*, *36*(4), 1105–1124.
Zhou, C., Wang, M., Zelinka, M., Liu, Y., Dong, Y., & Armour, K. (2023). Explaining forcing efficacy with pattern effect and state dependence. *Geophysical Research Letters*, *50*(3), e2022GL101700.
Zhou, C., Zelinka, M. D., & Klein, S. A. (2016, Dec 01). Impact of decadal cloud variations on the earth's energy budget. *Nature Geoscience*, *9*(12), 871-874. Retrieved from https://doi.org/10.1038/ngeo2828 doi: 10.1038/ngeo2828
Zhou, C., Zelinka, M. D., & Klein, S. A. (2017). Analyzing the dependence of global cloud feedback on the spatial pattern of sea surface temperature change with a green's function approach. *Journal of Advances in Modeling Earth Systems*, *9*(5), 2174–2189.
Zhu, J., & Poulsen, C. J. (2020). On the increase of climate sensitivity and cloud feedback with warming in the community atmosphere models. *Geophysical Research Letters*, *47*(18), e2020GL089143. doi: https://doi.org/10.1029/2020GL089143
Zhu, J., Poulsen, C. J., & Tierney, J. E. (2019). Simulation of eocene extreme warmth and high climate sensitivity through cloud feedbacks. *Science Advances*, *5*(9). doi: https://doi.org/10.1126/sciadv.aax1874

Supporting Information for "Non-monotonic feedback dependence on CO_2 due to a North Atlantic pattern effect"

Ivan Mitevski[1], Yue Dong[2], Lorenzo Polvani[1,2], Maria Rugenstein[3], Clara Orbe[1,4]

[1]Department of Applied Physics and Applied Mathematics, Columbia University, New York, NY

[2]Lamont-Doherty Earth Observatory, Columbia University, Palisades, NY

[3]Department of Atmospheric Science, Colorado State University, Fort Collins, CO

[4]NASA Goddard Institute for Space Studies, New York, NY

Contents of this file

Figures S1-S4.

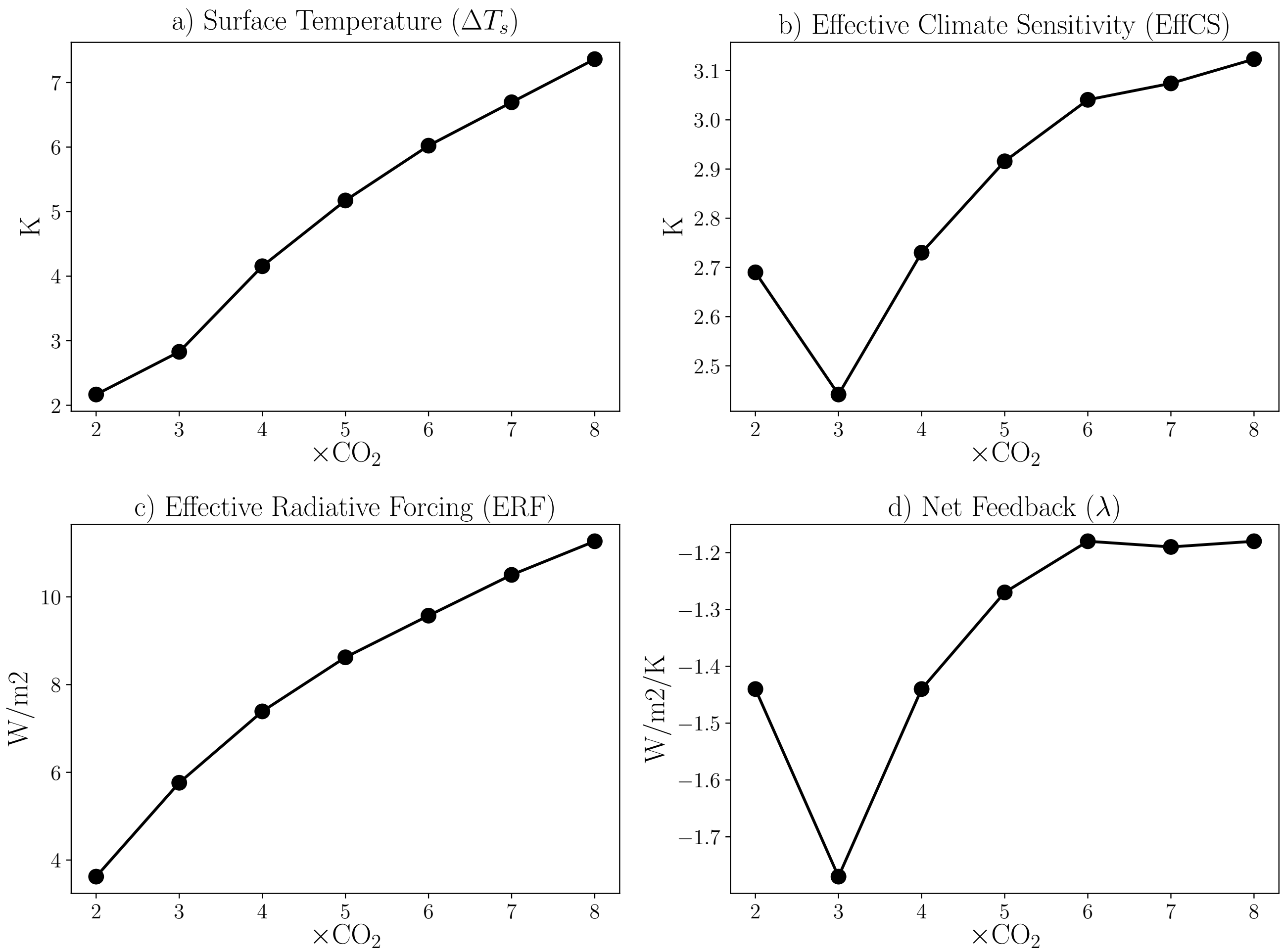

Figure S1. Same as Figure 1 in main text but for the GISS-E2.1-G model.

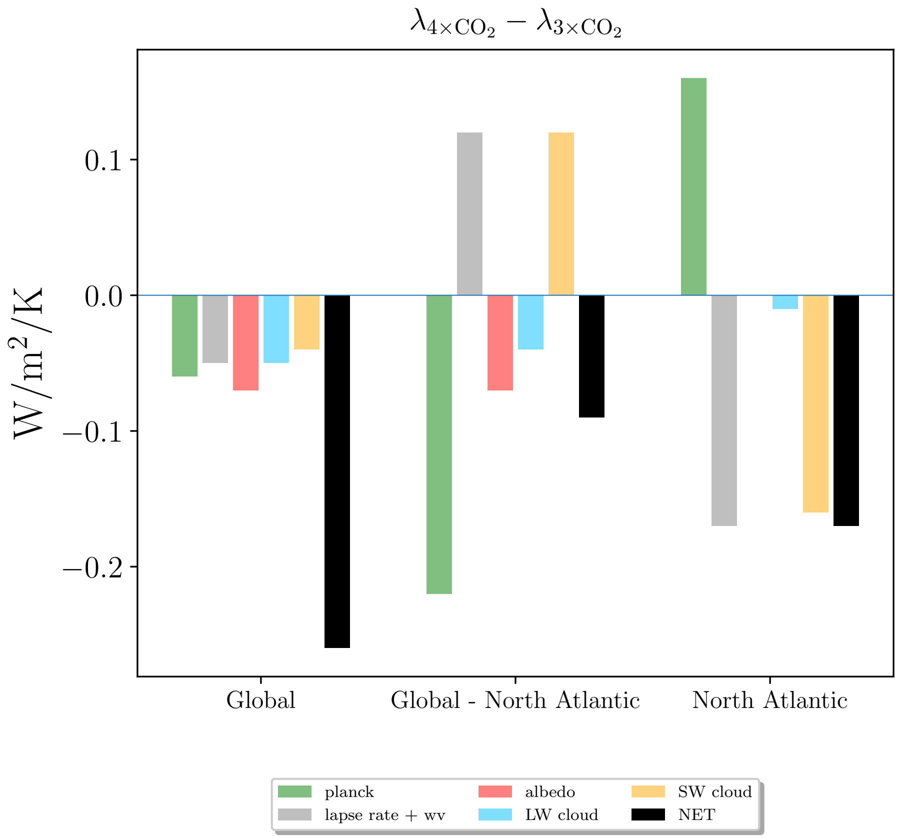

Figure S2. Individual feedback difference between $4\times CO_2$ and $3\times CO_2$ for Global, Global - North Atlantic, and the North Atlantic region. The North Atlantic is defined as a box between 0 to 60N and 80W to 10E.

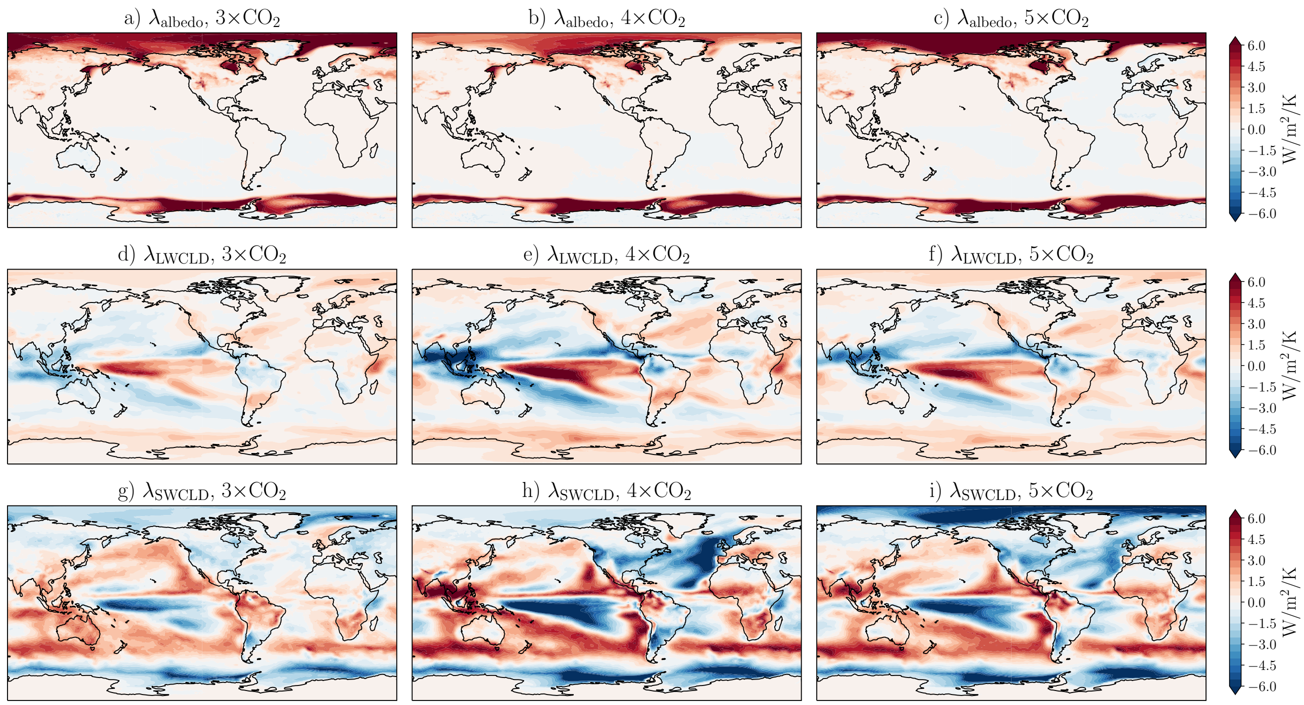

Figure S3. Maps of individual feedbacks calculated from prescribed-SST runs for: a-c) albedo, d-f) longwave cloud, and g-i) shortwave cloud.

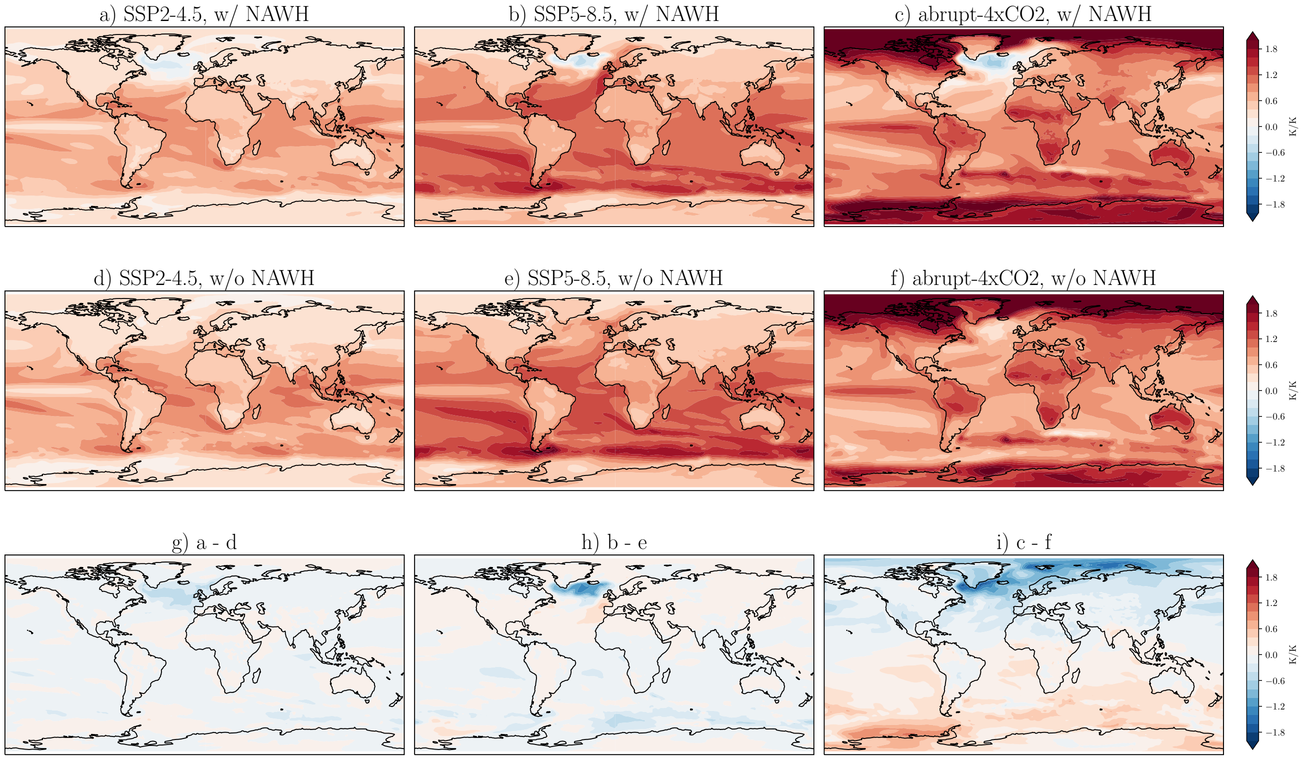

Figure S4. Maps of surface temperature patterns from two CMIP6 models composites with (a,b,c) and without (d,e,f) North Atlantic Warming Hole (NAWH), defined as cooling in the North Atlantic, and the difference (g,h,i). Composites are shown for SSP2-4.5 (a,d,g), SSP5-8.5 (b,e,h), and abrupt-4xCO2 scenario (c,f,i). The models without NAWH are ACCESS-CM2, AWI-CM-1-1-MR, CAMS-CSM1-0, CMCC-CM2-SR5, CanESM5, INM-CM4-8, IPSL-CM6A-LR, MIROC6, MPI-ESM1-2-HR, MPI-ESM1-2-LR. Models with NAWH are BCC-CSM2-MR, CESM2-WACCM, FGOALS-g3, GFDL-ESM4, IITM-ESM, KACE-1-0-G, MRI-ESM2-0, NorESM2-MM, TaiESM1. The surface temperature patterns are calculated as local surface temperature changes regressed to global surface temperature response for years 2015 to 2100 for the SSP scenarios and the first 150 years of the abrupt-4xCO2 runs, and then averaged across models.